

Title	The Orientation of Crystal Planes in Polyethylene Crystallized under Compression (Special Issue on Polymer Chemistry X)
Author(s)	Hyon, S.-H.; Taniuchi, H.; Kitamaru, R.
Citation	Bulletin of the Institute for Chemical Research, Kyoto University (1973), 51(2): 91-103
Issue Date	1973-08-06
URL	<a href="http://hdl.handle.net/2433/76481">http://hdl.handle.net/2433/76481</a>
Right	
Type	Departmental Bulletin Paper
Textversion	publisher

## The Orientation of Crystal Planes in Polyethylene Crystallized under Compression

S.-H. HYON, H. TANIUCHI, and R. KITAMARU\*

*Received April 12, 1973*

The orientations of the crystal planes (200) and (110) appearing in a lightly cross-linked polyethylene when its molten specimen is compressed between two metal plates are studied with three different X-ray techniques. It is confirmed that the (200)-orientation parallel to the film surface of the sample first appears at a relatively low degree of compression and the (110)-orientation follows at higher degrees of compression. These two kinds of orientation for the crystal planes were also observed for polyethylene samples through procedures involving two-dimensional stretching of molecular chains.

In a recent paper,<sup>1)</sup> it was manifested that, if a lightly cross-linked polyethylene film was compressed between two metal plates to high extents at the molten state and crystallized by cooling to room temperature, the crystal planes (200) and (110) parallel to the film surface appeared in the structure. This parallel orientation of the crystal planes was also recognized<sup>2)</sup> for a linear polyethylene without cross-linkings when it was biaxially stretched at high temperatures below its melting temperature.

This dual crystalline structure of polyethylene will have been brought about by the extreme anisotropy of the molecule and reflect a unique character for the crystallization of the polymer. Therefore, more detail cognition of this phenomenon, if the structure appears only under conditions mentioned above, will be of great importance in considering and elucidating the general mechanism for the crystallization of the polymer through different procedures.

In this paper, when a lightly cross-linked polyethylene film is compressed between two metal plates to different extents in the molten state and cooled to room temperature, the appearance of the two kinds of parallel orientation is separately examined. Furthermore, considering that the polymer molecules are subjected to a high extension in a two-dimensional direction during the compression or the biaxially stretching cited above to give the dual parallel orientation of the crystal planes, possibility to produce a similar orientation of the crystal planes through other processes such as rolling or calendaring that may involve two-dimensional stretching of molecules is inquired.

### EXPERIMENTAL

#### Preparation of Samples

A commercial high density polyethylene from Hoechst with a viscosity average molecular weight of  $2.5 \times 10^6$  was used in this study. A lightly cross-linked sample was

\* 玄 丞然, 谷内 秀夫, 北丸 竜三: Laboratory of Fiber Chemistry, Institute for Chemical Research, Kyoto University, Uji, Kyoto.

made by irradiation of this material with  $\gamma$ -ray from  $^{60}\text{Co}$  and compressed between two metal plates at the molten state to different extents in a similar manner described previously<sup>1)</sup>. Films about 1.5-mm thick of the polymer was irradiated to a dose of 2.7 megarads in vacuum at room temperature. The gel fraction (mass fraction of the nonsoluble part to the total mass) of this irradiated sample was 0.9 and the densities of cross-linked units and the free end groups were evaluated approximately to be  $1.8 \times 10^{-4}$  and  $1.1 \times 10^{-5}$ , respectively. The cross-linked sample was next compressed to different extents between two metal plates at 160–180°C and crystallized by cooling to room temperature over a period of 15 minutes. In this procedure, the film thicknesses were reduced in accord with the increase of the degree of compression. The degree of compression was expressed by the ratio between the film thicknesses before and after compression. The orientation of the crystal planes in these samples was studied by three X-ray diffraction techniques discribed later.

Uncross-linked material without irradiation was also used for other purposes. The film about 1.5-mm thick of the uncross-linked material was rolled with a rolling machine. The film was rolled at different temperatures between two rollers of 10-cm diameters that were rotating with a surface speed of 4 m/min. The clearance between two rollers was controlled so that the film thicknesses decreased to about 1/3 of the original thicknesses while holding at constant width. The crystal structure of samples was examined by a flat camera X-ray technique described later.

### Orientation of the Crystal Planes

The crystalline structure of samples was inquired with three different X-ray techniques.

**Method 1** The radiograph was taken with a flat camera with Ni-filtered Cu- $K_{\alpha}$  radiation. The X-ray beam was introduced to samples, either parallel or perpendicular to the sample films.

**Method 2** To study the spatial orientation of crystal planes, an X-ray scan was made in a manner previously described in detail.<sup>1)</sup> The diffraction intensity from the crystal planes (110), (200), (020), and (011) was recorded by a proportional counter that was set at an angle of  $2\theta$  for the each crystal plane against the incident beam. During this scan, samples were rotated so that the normal to the sample films  $N_f$  was rotated around the outer bisector of the incident and diffractive beams to the counter, starting from the position of the inner bisector of the beams to  $90^\circ$  (see Fig. 1). The diffraction intensity  $I(\phi)$  thus recorded for the each crystal plane as a function of the rotating angle  $\phi$  was multiplied by

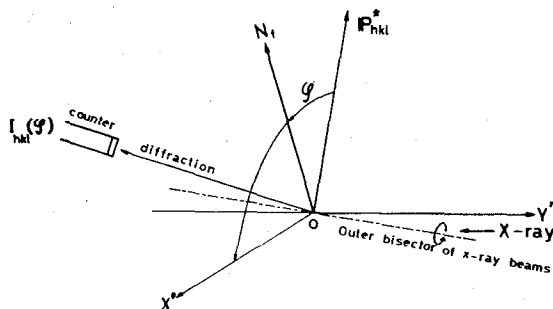


Fig. 1 Geometry for an X-ray scan (Method 2).

$\sin \phi$ . Since crystallites in samples are randomly distributed around the normal to the sample film independently of the compression ratio, the product  $I(\phi) \sin \phi$  evaluated for each crystal plane is indicative of the density of the probability that the vector  $P^*_{hkl}$  in an arbitrarily chosen crystallite points to the direction between  $\phi$  and  $\phi + d\phi$ .

**Method 3** Another X-ray scan was made in a similar manner as a routine scan for crystals of monomeric substances to identify those macroscopic surfaces. The diffraction was recorded with the proportional counter rotated around an axis perpendicular to both of the incident beam and the normal to the sample film  $N_f$  while the sample was also rotated around the same axis. The counter and the  $N_f$  were first set at angles of zero and  $90^\circ$  against the incident beam respectively and rotated so that the rate of the rotation for the former was twice that for the later.

The intensity thus recorded at angles of  $2\theta$  where  $\theta$  corresponds to each Bragg's angle for crystal planes is diffractions from the crystal planes parallel to the film surface of samples. In this scan, therefore, one can know what kind of crystal planes in the samples is parallel to the film surface.

## RESULTS AND DISCUSSION

### I The Crystal Plane Orientation of the Lightly Cross-linked Sample Crystallized under the Compressions

*Studies with the Method 1:* X-ray diffraction photographs were taken for samples with the compression ratios of 1, 3, 4, 5, 6, 8, and 10 with a flat camera. When the X-ray beam was introduced to samples perpendicular to the film surface of samples, the X-ray pattern obtained was composed of uniform circular rings for all samples. This indicates a random distribution of crystalline phases or crystal planes in the samples around the normal to the sample film (uniaxial random distribution around the normal  $N_f$ ), independent of the degree of compression. On the other hand, when the photograph was taken with an X-ray beam parallel to the film surface, very enhanced change in the pattern was observed depending on the degree of compression. The X-ray patterns shown in Fig. 2 manifest the change in the diffraction intensity in each circular diffraction for crystal planes (110), (200), (210), and (020).

Before considering these patterns, we must note the spatial geometry for the X-ray diffraction by the flat camera technique. Since an X-ray beam is introduced to samples from a direction parallel to the film surface and a sensitive film perpendicular to the incident beam is exposed to the diffractive beam, its geometry can be shown by Fig. 3. To consider the spatial distribution of crystal planes in samples, we assume here that vector  $P^*_{hkl}$  which represents the crystal plane (hkl) in the reciprocal lattice coordinate is statistically distributed in space. Then, a diffraction circle on the X-ray film defined by the Bragg's angle for a crystal plane considered is caused by the vectors  $P^*_{hkl}$  that make an angle of  $\pi/2 - \theta$  to the X-ray incident beam. In addition, the diffraction at the point D defined by an angle of  $\Omega$  on the circle is caused by the vectors  $P^*_{hkl}$  that further make an angle of  $\phi$  to the normal to the sample film. Here,  $\phi$ ,  $\Omega$  and the Bragg's angle  $\theta$  are correlated each other with an equation,

$$\cos \phi = \cos \theta \cos \Omega \quad (1)$$

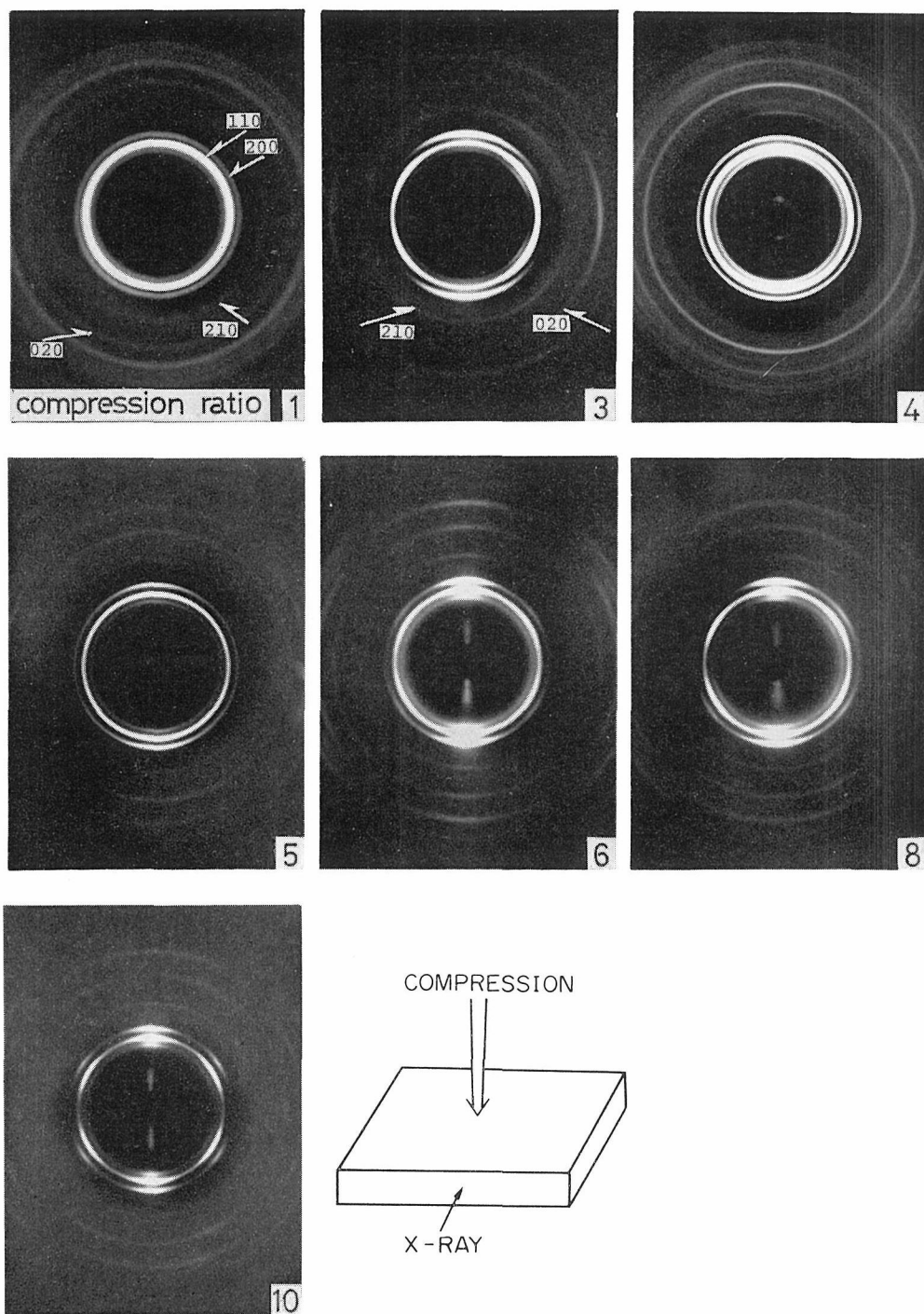


Fig. 2. X-ray patterns for the cross-linked sample. The compression ratios are indicated each patterns. To detect the (210)- and (020)-diffraction, the inner part of the sensitive film including the (110)- and (200)-diffractions were somewhat covered.

### Orientation of Crystal Planes in Polyethylene

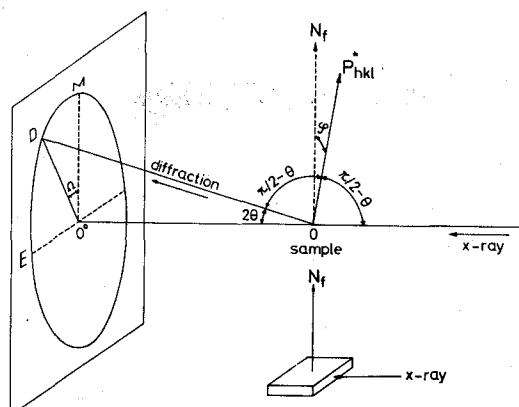


Fig. 3. Geometry for a flat camera X-ray technique (Method 1).

Therefore, the diffraction patterns obtained by the flat camera can be considered in terms of the spatial distribution of the crystal planes distributed in samples. Since a dual orientation of the crystal planes (200) and (110) parallel to the film surface appears at the higher compression ratios,<sup>1)</sup> we first consider a hypothetical diffraction pattern when either crystal plane  $P_{200}^*$  or  $P_{110}^*$  is oriented preferentially parallel to  $N_f$ . Then the points diffracted on the flat camera from each crystal plane can be easily calculated with use of the eq. (1) for both orientations.

If either  $P_{200}^*$  or  $P_{110}^*$  is located parallel to  $N_f$  in a crystallite, then the angles of  $P_{110}^*$ ,  $P_{200}^*$ ,  $P_{210}^*$ , and  $P_{020}^*$  to  $N_f$ ; namely the angle  $\phi$  in the eq. (1) for each crystal plane in either case, can be easily evaluated by referring to the reciprocal lattice of the orthorhombic crystal form of polyethylene. Using the angle  $\phi$  obtained in this manner with proper

Table I. The Diffractive Points from Various Crystal Planes on the Flat Camera for (110) and (200) Parallel Orientation to  $N_f$

(hkl)	$\Omega$ , degree	
	$P_{200}^*/N_f$ (200)-orientation	$P_{110}^*/N_f$ (110)-orientation
110	55.6	67.0, (0)*
200	(0)*	55.4
210	34.0	12.4, 86.8
020	90.0	28.9

Values were calculated with the orthorhombic crystal form,  $a=7.410$ ,  $b=4.945$ ,  $c=2.548$  Å, and  $\lambda=1.5418$  Å. \* The imperfect parallel orientation of either  $P_{200}^*$  or  $P_{110}^*$  where  $P_{200}^*$  or  $P_{110}^*$  makes angle of each Bragg's angle with  $N_f$  ( $\varphi=0$ ) should result in diffractions on meridian ( $\Omega=0$ ) of each diffractive circular ring. The diffractions on the meridian are brought about by vectors that make an angle of  $\theta$  with  $N_f$ . Furthermore, it is to be noted that, if the c-axes are located parallel to the film surface and some crystallites are distributed randomly around the c-axes, the diffraction peak should more or less appear on the meridian for all (hk0)-crystal planes.

numerical values for  $\theta$  and the lattice parameters, the points diffracted on the flat camera in both cases of the orientations was determined by the eq. (1). The results are listed in Table I as values of  $\Omega$ . Now consider the significance of the X-ray patterns shown in Fig. 2. At a compression ratio of 3, the intensity of the (110)-diffraction decreases in both meridional and equatorial directions, showing diffuse four points maxima at intermediate angles. The (200)-diffraction converges into the meridional directions, losing its intensity at the equatorial and intermediate angles. Table I suggests that the (200)-orientation gives an enhanced intensity at the  $\Omega$ -angles of 55.6 and zero for the (110)- and (200)-diffractions, respectively. Hence, correspond to  $\Omega$  angles appeared for each diffraction, the (200)-orientation should be thought to have already appeared by the compression ratio of 3. On the other hand, since no enhanced intensity is observed at the  $\Omega$ -angle of zero for the (110)-diffraction, it is thought that the (110)-orientation has not appeared as yet by this compression ratio.

As the compression ratio increases beyond 3, significant change in the X-ray patterns is recognized. The four points maxima observed for the (110)-diffraction at the compression ratio of 3 become obscure again by gradual increases in the diffraction intensity at the meridional angles. Beyond the compression ratio of 6, the (110)-diffractions converge to six points at the intermediate and meridional angles, this six points pattern becoming to be very explicit by the final compression ratios of 8 and 10.

For the (200)-diffraction, it is observed that the intensity at the intermediate angles lost at the compression ratio of 3 recovers and converges to four maxima as the compression ratio increases from 4 to 5, emphasizing its intensity on the meridian beyond the compression ratio of 6 to 10. At the highest compression ratios six maxima are explicit, two of those being on the meridian.

The above-mentioned change in the X-ray patterns by further increase of the compression ratio beyond 3 will be explained by gradual occurrence of the (110)-orientation in addition to the (200)-orientation that has appeared in ahead at the compression ratio of 3. The diffuse four points maxima for the (110)-diffraction at the compression ratio of 3 by the (200)-orientation would become obscure as the compression ratio increased to 4 and 5 by gradual increase in the intensity at  $\Omega=0$  and 67.0, which were caused by the gradual appearance of the (110)-orientation. The distinct six points maxima for the (110)-diffraction observed at the compression ratios larger than 6 will be caused by rather perfect orientations of both crystal planes, (200) and (110). The two maxima on the meridian will be originated by the imperfect (110)-orientation, and the four maxima will be composed of superposed maxima, each of which is at  $\Omega=55.6$  and 67.0 by the (200)- and (110)-orientations, respectively.

Also the (110)-orientation will be responsible for the four points maxima of the (200)-diffraction at the intermediate angles around  $\Omega=55.4^\circ$  that is originated at a compression ratio of 4 or 5 and established distinctly at compression ratios beyond 6.

The diffractions from the crystal planes (210) and (020) were not seen clearly in the printed patterns in the text, but examining of those original patterns gave some information of the crystal planes orientation. The (210)-diffraction lost its intensity in both meridional and equatorial directions at a compression ratio of 3, but after indicating a spurious uniform circular distribution at the intermediate compression ratios the diffractions tended to converge into rather lower angles of  $\Omega$  and the equatorial angles. The (020)-diffraction

### Orientation of Crystal Planes in Polyethylene

indicated an enhanced intensity on the equator at a compression ratio of 3, and at the highest compression ratio it also exhibited enhanced intensity at lower angles of  $\Omega$  around  $28.9^\circ$ . The above-mentioned observations for the (210)- and (020)-diffractions can be also understood by progressive appearance of the (200)- and (110)-orientation of the crystal planes.

Thus all informations of the diffraction patterns for the (110), (200), (210) and (020) crystal planes lead a conclusion that during the crystallization under the two-dimensional compression the (200)-orientation first appears at a relatively low compression ratio and the (110)-orientation follows at the higher compression ratios.

*Studies with the Method 2:* The conclusion reached above can be further confirmed by the studies with the second technique of X-ray diffraction. The products  $I(\phi) \sin \phi$  for the (110)-, (200)-, (020)-, and (011)-diffractions for the samples with different compression ratios are plotted against  $\phi$  in Figs. 4, 5, 6, and 7, respectively. This product indicates the probability density that the vector  $P^*$  for each crystal plane points to the direction between  $\phi$  and  $\phi + d\phi$  in an arbitrarily chosen crystallite in samples as mentioned before. Hence, one can inquire the appearance of the crystal plane orientations with the increase of the compression ratio by examining these figures.

In each figure, the peak positions when either (200)- or (110)-orientation appears are

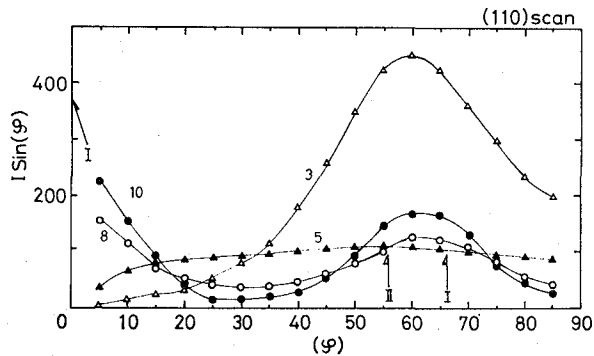


Fig. 4.  $\sin \phi I(\phi)$  vs.  $\phi$  for (110) for the cross-linked sample: compression ratio, 3-open triangle, 5-closed triangles, 8-open circles, 10-closed circles. Arrow I indicates the peak position for the (110)-orientation and II indicates that for the (200)-orientation.

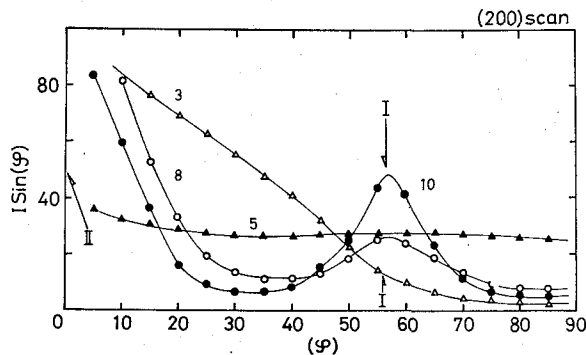


Fig. 5.  $\sin \phi I(\phi)$  vs.  $\phi$  for (200). See the legend for Fig. 4 for triangles, circles and arrows.



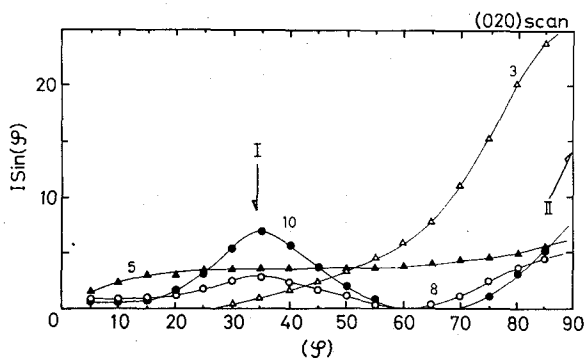


Fig. 6.  $\text{Sin } \phi I(\phi)$  vs.  $\phi$  for (020). See the legend for Fig. 4 for triangles, circles and arrows.

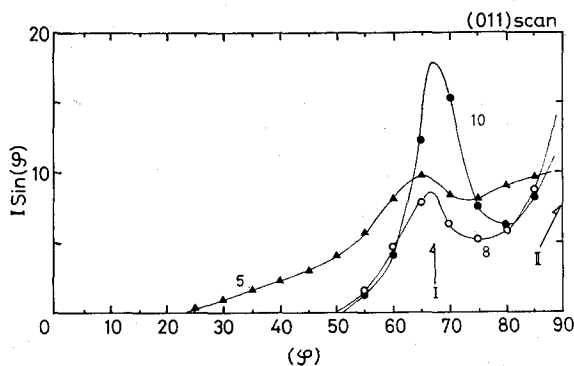


Fig. 7.  $\text{Sin } \phi I(\phi)$  vs.  $\phi$  for (011). See the legend for Fig. 4 for triangles, circles and arrows.

indicated by the arrows II and I, respectively. In the each figure intensity peaks are recognized at the angles of  $\phi$  that correspond to the arrow II for the sample with a compression ratio of 3. After these peaks becoming obscure at a compression ratio of 5, the peaks become to be distinctly recognized at the angles of  $\phi$  that correspond to both of the arrows II and I as the compression ratios increase from 8 to 10. These results support the conclusion reached above by the flat camera X-ray technique that the (200)-orientation appears at the low compression ratio of 3 and the (110)-orientation follows as the compression ratio increased and at the highest compression ratio rather perfect plane orientations of both kinds coexist in the crystalline structure of samples.

*Studies with the Method 3:* The progressive appearance of the (200)- and (110)-parallel orientations with the increase of the compression ratio can be verified semi-quantitatively with the technique 3. In Fig. 8 the diffraction intensity for the samples with the compression ratios of 1, 3, 5, 8 and 10 is plotted against  $2\theta$ , the angle of the proportional counter to the incident beam. Since the diffractive beam recorded in this manner of scan is responsible only for the crystal planes that are parallel to the film surface of the sample as described in the experimental section, the relative ratio between the intensities at the angles of  $2\theta$ ; that correspond to twice of the Bragg's angle for the (200) and (110) crystal planes will be indicative of the relative mass ratio between the two orientations.

### Orientation of Crystal Planes in Polyethylene

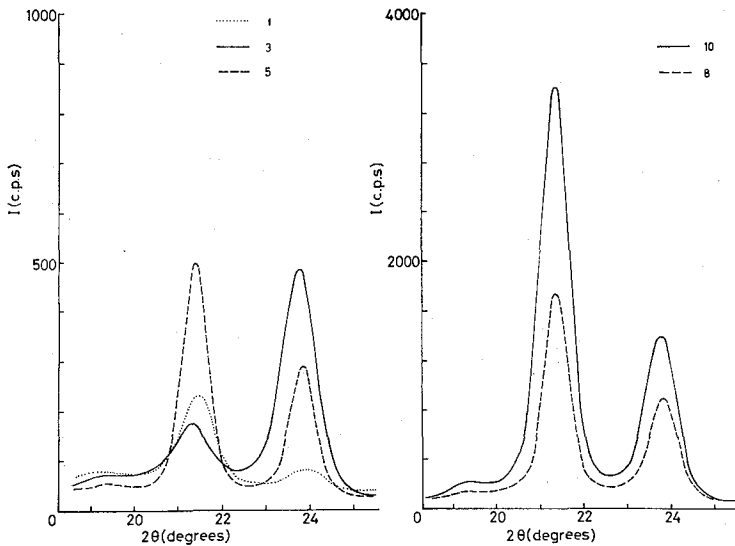


Fig. 8. X-ray scan (Method 3) for the cross-linked sample with different compression ratios. The compression ratios are indicated in each curve.

When the crystallites in samples are randomly distributed in space, it is known by the data for the sample with a compression ratio of 1 (not compressed) and by an early work of Bunn<sup>3)</sup> that the intensity ratio of the (110)-diffraction to the (200)-diffraction at each  $2\theta$  angle is in an order of 4-5. However, the intensity ratio is significantly altered in accord with the increase of the compression ratio. This quantity was determined from the data in the figure with use of proper baselines for each curve and listed in the second column in Table II.

If we designate  $I_{110}$  and  $I_{200}$  for the diffraction intensity at each  $2\theta$ , the relative existence ratio  $E_{200/110}$  of the (200)- and (110)-orientations can be evaluated by,

$$\begin{aligned}
 E_{200/110} &= (I_{200}/I_{200}^{\circ}) / (2I_{110}/I_{110}^{\circ}) \\
 &= (I_{110}^{\circ}/2I_{200}^{\circ}) / (I_{110}/I_{200})
 \end{aligned}
 \tag{2}$$

Table II. The Intensity Ratio between the (110)- and (200)-Diffractions and the Relative Existence Ratio between the (200)- and (110)-Orientations for Samples with Different Compression Ratios.

Compression ratio of samples	Intensity ratio $I_{110}/I_{200}$	Relative existence ratio between the (200)- and (110)-orientations $E_{200/110}$
1	4.56	—
3	0.295	7.73
5	1.78	1.30
8	2.26	1.00
10	2.53	0.90

Here,  $I_{110}^{\circ}$  and  $I_{200}^{\circ}$  are the quantities for the randomly oriented sample without compression. In Table II, the relative existence ratios evaluated in this manner are listed with the intensity ratio of the two kinds of diffractions.

The relative existence ratio of 7.73 much larger than unity at a compression ratio of 3 should be nothing but to exhibit firm appearance of the (200)-orientation at this compression ratio with absence of the (110)-orientation. The existence ratio decreases rather abruptly to 1.30 at a compression ratio of 5 and gradually decreases to 1.00 and 0.90 as the compression ratio increases to 8 and 10. This will mean that the (110)-orientation appears at a compression ratio of 5 to an extent to correspond with the (200)-orientation in quantity, and subsequently the both orientations progressively become to be enhanced and sharp without changing appreciably those relative quantities, so that the very characteristic X-ray patterns are obtained by the flat camera technique at the highest compression ratios.

## II. The Crystal Plane Orientation of Polyethylene Samples Made by Other Procedures

It has been firmly concluded that if the lightly cross-linked polyethylene is two-dimensionally compressed at the molten state and crystallized by cooling to room temperature, the (200)- and (110)-orientations progressively appear with the increase of the compression ratio. As pointed out in the introductory section, these crystal plane orientations may appear during procedures for polyethylene accompanying a high stretching of molecular chains.

The X-ray photographs were taken with the flat camera for various samples made by the rolling to study this phenomenon.

### The Lightly Cross-linked Sample

The lightly cross-linked sample was melted at 160°C and rolled at room temperature so that the film thickness was reduced to about 1/3 of its original thickness while holding at constant width, according to the procedure described in the experimental section. The X-ray diffraction photographs taken in the three directions are shown in Fig. 9. The patterns taken in the 1- and 2-directions show a  $c^*$ -axis orientation parallel to the machine direction. These two patterns may not give information of the orientation of crystal planes owing to those strong uniaxial orientation in the machine direction. However, the pattern taken in the 3-direction clearly shows firm existence of both (200)- and (110)-plane orientations parallel to the film surface of the sample in addition to the  $c^*$ -axis orientation. For the (110)-diffractions, intensity peaks are recognized in the meridional and intermediate directions. The intensity in these directions will respectively correspond to  $\Omega=0$  arising from the (110)-orientation and to  $\Omega=67.0$  and  $55.6^{\circ}$  (superposed) arising from the (110)- and (200)-orientations (refer Table I). Also for the (200)-diffraction enhanced intensity is recognized in the meridional and intermediate directions, that will correspond to  $\Omega=0$  and  $55.4^{\circ}$  arising from the (200)- and (110)-orientations respectively. Thus it is concluded that both (200)- and (110)-orientations exist in this sample.

### The Sample without Cross-linkings

The film of the uncross-linked polyethylene, when its molten specimen was compressed to a compression ratio of 10 between two metal plates at 130°C and quenched

## Orientation of Crystal Planes in Polyethylene

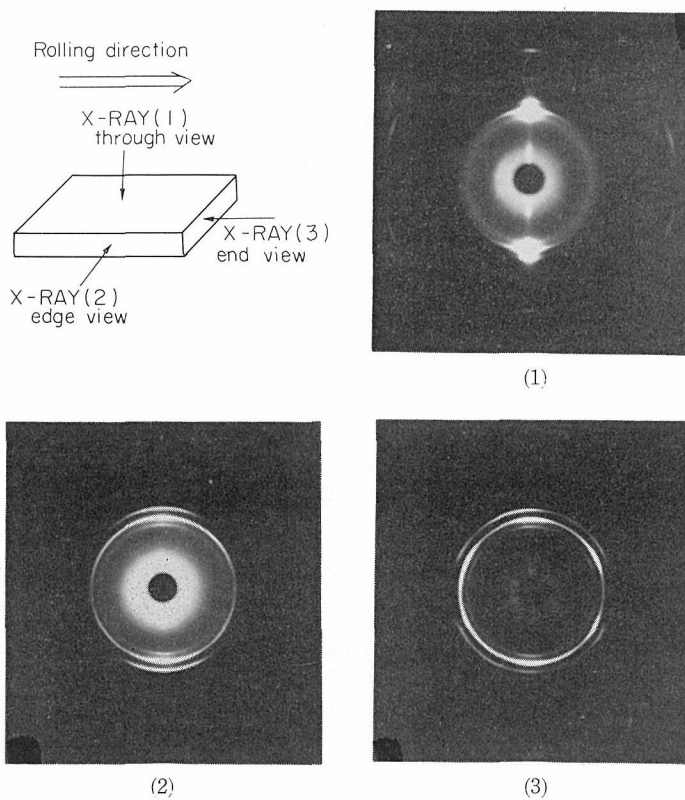
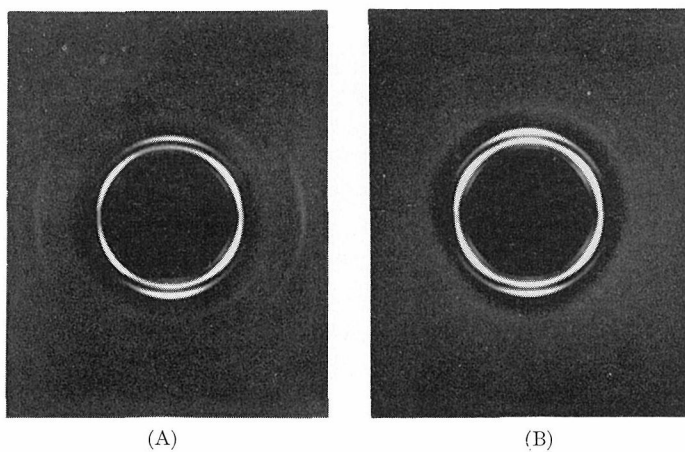


Fig. 9. The flat camera X-ray patterns for the cross-linked sample rolled at room temperature after premelting with X-ray incident beam in different directions.



A: Compressed 10 times at 130°C after premelting (Edge view),  
 B: Rolled at 80°C after premelting (Direction 3).

Fig. 10. The flat camera X-ray patterns for the uncross-linked sample.

to room temperature or it was rolled to about 2 times at about 80°C, exhibited X-ray diffraction patterns that indicate the (200)-orientation with either absence or minor presence of the (110)-orientation. The X-ray patterns for those samples are shown in Fig. 10. Here the patterns taken only in the direction 3 are shown, since those are adequate to consider the plane orientation. As can be seen, both patterns clearly indicate the existence of the (200)-orientation. But the contribution from the (110)-orientation is either not detected (the former sample) or very minor (the latter sample).

On the other hand, if the uncross-linked sample was rolled at temperatures lower than 80°C without premelting, an X-ray pattern to indicate existence of both (200)- and (110)-orientations was always obtained. X-ray patterns have been sometimes presented for polyethylene samples rolled at low temperatures up to date.<sup>4,5</sup> If one examines carefully those patterns, existence of the both crystal plane orientations could be easily confirmed. Take the figure 12-C in the reference (4) for instance. This is an X-ray pattern for a rolled polyethylene at room temperature when an X-ray beam is introduced from the machine direction. The existence of the both orientations will be easily confirmed by the (110)- and (200)-diffractions on the pattern referring to Table I (note here that the angle of  $\Omega$  in Table I corresponds to angles from the equator of this pattern).

#### SUMMARY AND UNIVERSAL DISCUSSION

It is confirmed by three X-ray techniques that a lightly cross-linked film is two-dimensionally compressed between two metal plates at the molten state and crystallized by cooling to room temperature, the orientation of the crystal planes (200) and (110) parallel to the film surface of the sample appears in the structure. Between these two orientations, the (200)-orientation first appears at a relatively low degree of compression such as 3 and the other follows at higher degrees of compression such as larger than 5, both becoming explicit and sharp progressively according to the increase of the degree of compression.

After appearing of both orientations, those are approximately comparable in mass so that the relative mass ratio between the (200)- and/ (110)-orientations gradually decreases from 1.30 to 0.90 as the compression ratio increases from 5 to 10.

This orientation of the crystal planes was also recognized for polyethylene undergone other procedures accompanying crystallization or re-crystallization under stretching of molecular chains, irrespective of the presence of cross-linkings. However, in these procedures both of the (200)- and (110)-orientations not necessarily take place but only one of two can occur sometimes. For example, both orientations take place for the lightly cross-linked sample when its molten specimen is rolled at room temperature. But if the uncross-linked sample is rolled at 80°C or its molten specimen is two-dimensionally compressed between two metal plates at 130°C and quenched to room temperature, only the (200)-orientation takes place. However, if the uncross-linked sample is rolled at temperatures lower than 80°C without premelting, both of the (200)- and (110)-orientations appear.

The foremost appearance of the (200)-orientation for the cross-linked sample when its molten specimen is two-dimensionally compressed will be significant in connection with the result obtained previously<sup>1</sup>) that this orientation is predominant than the (110)-orientation for a cross-linked polyethylene sample whose molecular chains are thought

to be more susceptible to the macroscopic deformation in the molten state. Based this result together with informations of the crystallites size of the sample,<sup>6)</sup> we previously assumed<sup>1)</sup> that the structure of the sample was composed of aggregations of plate-like crystallites, the planes of which are coincident with either the crystal plane (200) or (110). However with data obtained here, we further suggest that for the crystalline structure of the sample the plate-like crystallites whose planes coincide with the (200)-plane are originated by nucleation for the crystallization of the polymer under such conditions involving two-dimensional stretching of molecular chains. On the other hand, the origin of the other type of crystallites should be sought in other ways. At the present time we think that a partial destruction of the crystallites along the (110)-crystal planes could produce the other type of plate-like crystallites, the crystal planes of which are coincident with the (110)-plane. Otherwise, conditions for crystallization involving two-dimensional stretching of molecular chains under the very high hydrostatic pressure may produce a nucleation for the crystallization that gives this kind of plate-like crystallites.

The irradiation work in this study was done with a <sup>60</sup>Co source equipped in a Laboratory of Fiber Chemistry, Institute for Chemical Research, Kyoto University with help of Mr. T. Ikeda.

#### REFERENCES

- (1) R. Kitamaru, H.-D. Chu, and S.-H. Hyon, *Macromolecules*, **6**, 337 (1973).
- (2) G. C. Adams, *J. Polym. Sci., A-2*, **9**, 1235 (1971).
- (3) C. W. Bunn, *Trans. Faraday Soc.*, **35**, 482 (1938).
- (4) G. Meinel and A. Peterlin, *Kolloid-Z. Z. Polym.*, **242**, 1151 (1970).
- (5) M. Yamada, K. Miyasaka, and K. Ishikawa, The 20th Meeting of Soc. Polym. Chem. Japan, Tokyo, Nov. 1971, Preprints, No. 2, p. 835.
- (6) S.-H. Hyon and R. Kitamaru, to be published.